JACS
JOURNAL OF THE AMERICAN CHEMICAL SOCIETY
Article
pubs.acs.org/JACS

A Fluorescent Sensor for GABA and Synthetic $GABA_B$ Receptor Ligands

Anastasiya Masharina, Luc Reymond, Damien Maurel,[†] Keitaro Umezawa,[‡] and Kai Johnsson*

Institute of Chemical Sciences and Engineering (ISIC), Institute of Bioengineering, NCCR in Chemical Biology, Ecole Polytechnique Fédérale de Lausanne (EPFL), 1015 Lausanne, Switzerland

Supporting Information

ABSTRACT: While γ-aminobutyric acid (GABA) is the main inhibitory neurotransmitter, suitable tools to measure its concentration in living cells with high spatiotemporal resolution are missing. Herein, we describe the first ratiometric fluorescent sensor for GABA, dubbed GABA-Snifit, which senses GABA with high specificity and spatiotemporal resolution on the surface of living mammalian cells. GABA-Snifit is a semisynthetic fusion protein containing the $GABA_B$ receptor, SNAP- and CLIP-tag, a synthetic fluorophore and a fluorescent $GABA_B$ receptor antagonist. When assembled on cell surfaces, GABA-Snifit displays a GABA-dependent fluorescence emission spectrum in the range of 500−700 nm that permits sensing micromolar to millimolar GABA concentrations. The ratiometric change of the sensor on living cells is 1.8. Furthermore, GABA-Snifit can be utilized to quantify the relative binding affinities of $GABA_B$ receptor agonists, antagonists and the effect of allosteric modulators. These properties make GABA-Snifit a valuable tool to investigate the role of GABA and $GABA_B$ in biological systems.

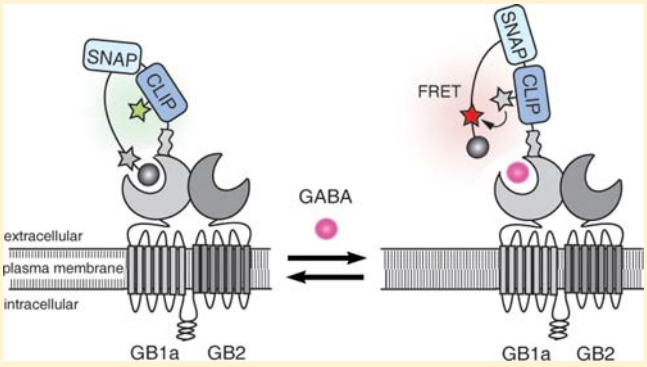

INTRODUCTION

γ-Aminobutyric acid (GABA) is the main inhibitory neurotransmitter in the mammalian nervous system.[1] Perturbations in GABAergic inhibition are responsible for neurological disorders such as epilepsy, anxiety disorders, and schizophrenia.[2] In addition to its role in neuronal communication, GABA plays a role in embryonic development and adult neurogenesis.[3] Furthermore, GABA participates in intercellular communication outside the nervous system.[4] A detailed characterization of the role of GABA in these different biological processes will require the measurement of GABA concentrations with high temporal and spatial resolution. Reported noninvasive methods for analysis of GABA concentrations in living systems are based on in vivo magnetic resonance spectroscopy (MRS)[5,6] and in vivo microdialysis techniques.[7,8] Furthermore, electrochemical[9] and piezoelectric[10] GABA sensors were developed to detect GABA ex vivo. However, these methods lack the required sensitivity or spatiotemporal resolution to measure GABA concentrations on the level of a single cell required for further elucidation of the role of GABA. Fluorescent biosensors based on Förster resonance energy transfer (FRET) are well suited for the measurement of small-molecule concentrations in cells and in vivo.[11] Such FRET biosensors are usually based on a receptor protein that undergoes a conformational change upon binding to the analyte of interest. Expressing such a receptor protein as a fusion protein with two autofluorescent proteins can then result in the generation of a FRET sensor. Despite successful examples of FRET sensors for the neurotransmitter glutamate,[12] carbohydrates,[13] cyclic nucleotides,[14,15] ATP, and others,[16−18] no FRET biosensors for GABA have been reported so far. Using traditional methods for the generation of FRET biosensors we would first need to identify an appropriate GABA binding protein which undergoes a significant conformational change upon GABA binding − so far none has been found. Recently, we reported an approach for the creation of FRET-based biosensors that circumvents the need for a conformational change of an analyte binding protein.[19−21] These sensors, termed Snifits (**SN**AP-tag based **i**ndicator with a **f**luorescent **i**ntramolecular **t**ether), are fusion proteins consisting of SNAP-tag, CLIP-tag, and a receptor protein (Figure 1A). SNAP- and CLIP-tag, two self-labeling protein tags,[22,23] are labeled with a synthetic fluorophore tethered to a receptor protein ligand and a second synthetic fluorophore, respectively. The ligand binds to the receptor protein and maintains the Snifit in a closed conformation. Free analyte competes for binding to the receptor protein and can shift the equilibrium toward an open conformation. The conformational change results in reduced proximity of the two fluorophores and hence a change in their FRET efficiency.

Here we introduce a Snifit for GABA that is based on the metabotropic $GABA_B$ receptor as a receptor protein and a fluorescent antagonist as a synthetic ligand (Figure 1B). GABA-Snifit represents the first biosensor that permits the measure-

Received: June 28, 2012
Published: October 24, 2012

   dx.doi.org/10.1021/ja306320s | J. Am. Chem. Soc. 2012, 134, 19026−19034

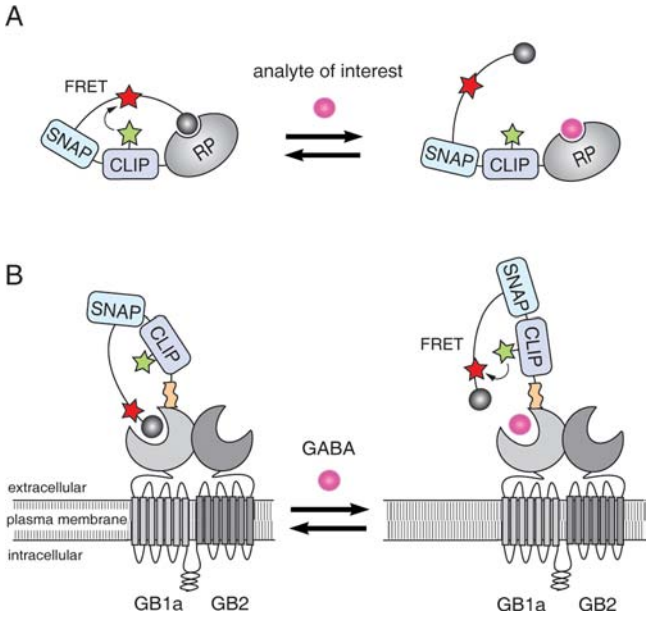

Figure 1. Snifits. (A) Snifit principle. A Snifit is composed of a fusion protein between SNAP-tag, CLIP-tag, and a receptor protein (RP) for the analyte of interest. SNAP-tag is labeled with a molecule containing a fluorophore (red star) and a ligand (gray ball) that binds to the RP; CLIP-tag is labeled with a second fluorophore (green star). In the absence of analyte (pink ball), the intramolecular ligand keeps the Snifit in a closed conformation. In the presence of sufficient concentrations of analyte, the Snifit is shifted toward an open conformation. Opening and closing of the Snifit are detected through changes in FRET efficiency between the two fluorophores. (B) GABA-Snifit. The metabotropic $GABA_B$ receptor composed of the GB1a (light gray; containing the sushi domains (orange)) and the GB2 subunit (dark gray) is used as RP and a $GABA_B$ receptor antagonist (gray ball) as intramolecular ligand. GABA-Snifit detects GABA or synthetic $GABA_B$ ligands through displacement of the intramolecular antagonist and a resulting change in FRET efficiency. As $GABA_B$ is known to form oligomers on cell surfaces, it should be noted that an intermolecular binding of the tethered antagonist cannot be excluded.

ment of GABA concentrations on the surface of mammalian cells with high temporal and spatial resolution.

RESULTS

Design of GABA-Snifit. The design of a Snifit for GABA requires a suitable GABA-binding protein as well as a synthetic ligand that competes with GABA for binding to the receptor. For the GABA-binding protein we chose the metabotropic G protein-coupled $GABA_B$ receptor. The $GABA_B$ receptor is an obligatory heterodimeric transmembrane receptor composed of the homologous subunits $GABA_{B1}$ (GB1) and $GABA_{B2}$ (GB2). Furthermore, two GB1 receptor isoforms resulting from alternative splicing exist, GB1a and GB1b. GB1a contains two N-terminal complement control protein (CCP) modules, the so-called sushi domains (SDs) that are lacking in GB1b.[24] The SDs are conserved protein interaction motifs which are believed to be important for axonal targeting of the receptor.[25] Both subunits GB1 and GB2 possess a large extracellular domain, the so-called venus flytrap domain (VFT) which is linked to the N-terminus of a heptahelical transmembrane domain (7TM). The VFT of GB1 binds orthosteric ligands such as GABA and other agonists or antagonists, whereas the VFT of GB2 does not bind any orthosteric $GABA_B$ receptor ligand.[26] Upon agonist binding, the two lobes of GB1 VFT close. This results in a change in the relative orientation of the two subunits and to G protein activation by the 7TM of GB2.[27] It has been shown that SNAP-tag fusion proteins of the $GABA_B$ receptor are functional and have been used for FRET studies on receptor dimerization in living cells.[28] For the generation of GABA-Snifit we focused on GB1a and generated a construct for the expression of a SNAP-CLIP-GB1a fusion protein (Figure 1B). Functional GABA-Snifit then is based on the coexpression of SNAP-CLIP-GB1a and GB2, and the labeling of the sensor with a fluorescent ligand that competes with GABA for binding.

Various $GABA_B$ receptor agonists and antagonists have been reported,[29] and some of these were derivatized with synthetic probes without abolishing their binding affinity to the receptor.[29−31] For the labeling of GABA-Snifit, antagonists are preferable over agonists as they keep the G protein-coupled receptor (GPCR) in an inactive state. We therefore chose the $GABA_B$ receptor antagonist CGP 51783 **1** ((3-[[4-chlorophenyl)methyl]amino-propyl]-(P-diethoxymethyl)-phosphinic acid) as a starting point for the generation of a fluorescent ligand (Figure 2A).[32] The affinity of CGP 51783 has been reported to be 1 μM. Furthermore, it has been shown that coupling of a similar antagonist to a spacer did not affect its affinity to $GABA_B$.[31] This suggests that tethering of compound **1** to SNAP-tag should not disrupt its binding affinity. To transform CGP 51783 **1** into an appropriate substrate for GABA-Snifit, we synthesized derivative **2** (Figure 2A) to which fluorophores and the SNAP-tag substrate benzylguanine (BG) were coupled via a short flexible linker (Figure 2B). The resulting probes BG-Cy5-CGP **3**, BG-TMR-CGP **4**, and BG-AlexaFluor594-CGP **5** contained a polyethylene glycol (PEG) linker between BG and the fluorophore to facilitate binding of the antagonist to the receptor. For control experiments we prepared the identical SNAP-tag substrates but lacking the $GABA_B$ receptor antagonist (BG-Cy5 **6**, BG-TMR **7**, and BG-AlexaFluor594 **8**; Figure S1(Supporting Information [SI]). A detailed outline of the synthesis of all derivatives is provided in the SI.

Characterization of GABA-Snifit. To confirm the cell surface expression of GABA-Snifit, human embryonic kidney 293 cells (HEK 293 cells) transiently expressing SNAP-CLIP-GB1a and GB2 were labeled with fluorescent substrates of SNAP- and CLIP-tag and subsequently analyzed by confocal fluorescence microscopy (Figure 3A). These data demonstrate that GABA-Snifit is well expressed and can be specifically labeled via SNAP-tag and CLIP-tag. Furthermore, the cell lysate of cells expressing SNAP-CLIP-GB1a and GB2 was analyzed by sodium dodecyl sulfate polyacrylamide gel electrophoresis (SDS-PAGE) and subsequent in-gel fluorescence scanning, demonstrating the presence of doubly labeled sensor proteins of the correct size (Figure 3B).

We then investigated if GABA-Snifit retains the affinity of native $GABA_B$ receptor for GABA and is capable of GPCR signaling. To detect GABA-binding and receptor activation of GABA-Snifit, we coexpressed SNAP-CLIP-GB1a, GB2, and the chimeric G protein Gqi9 in HEK 293 cells and analyzed the nonlabeled GABA-Snifit. It has been previously shown that Gqi9 permits activation of phospholipase C (PLC) by the $GABA_B$ receptor in HEK 293 cells.[33] Active PLC stimulates inositol 1,4,5-trisphosphate (IP_3) formation which triggers calcium release from the endoplasmic reticulum (ER) into the cytosol. Upon addition of different GABA concentrations we measured an increase in cytosolic calcium concentrations utilizing a calcium-sensitive fluorescent dye. We analyzed

dx.doi.org/10.1021/ja306320s | J. Am. Chem. Soc. 2012, 134, 19026−19034

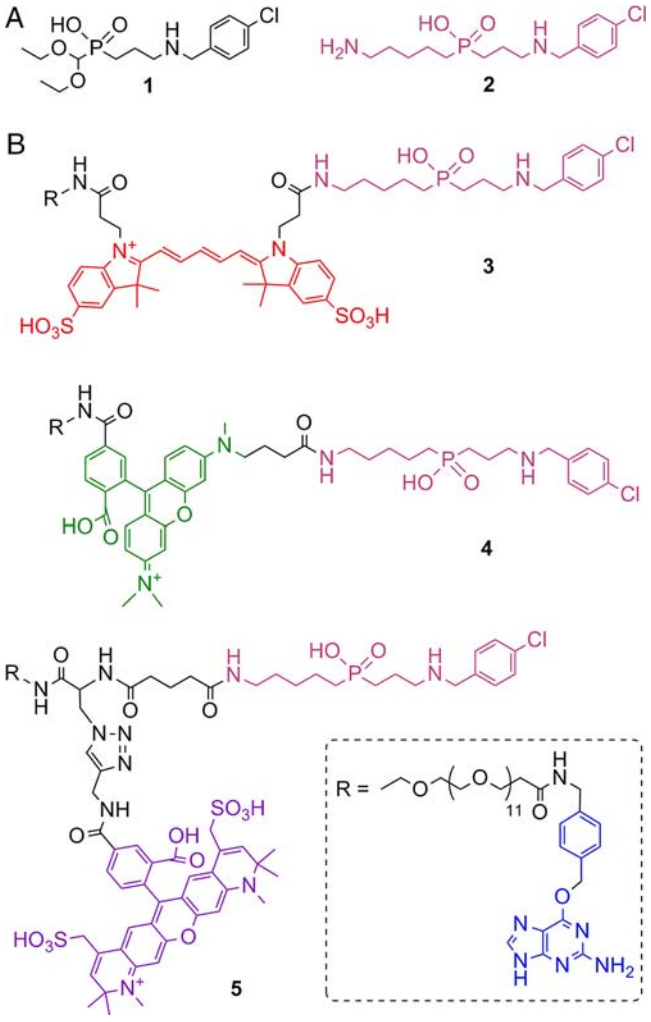

Figure 2. Molecules used for labeling of GABA-Snifit. (A) $GABA_B$ receptor antagonist CGP 51783 **1** and its derivative **2** used for generation of tethered fluorescent ligands. (B) Synthetic probes for semisynthesis of GABA-Snifit; these probes contain the SNAP-tag substrate benzylguanine (BG) (blue), the intramolecular ligand CGP (pink), and different fluorophores. Top: BG-Cy5-CGP **3** (red). Middle: BG-TMR-CGP **4** (green). Bottom: BG-AlexaFluor594-CGP **5** (violet).

PLC activation as a function of [GABA] and obtained a half maximal effective concentration (EC_{50}) of 56 ± 19 nM for GABA-Snifit (Figure 3C). This value describes the GABA concentration that results in a half maximal calcium response in cells transiently expressing GABA-Snifit. These data demonstrate that GABA-Snifit binds GABA and is functional with respect to GPCR signaling.

Measuring GABA with GABA-Snifit. To test the suitability of GABA-Snifit for GABA sensing, HEK 293 cells coexpressing SNAP-CLIP-GB1a and GB2 were labeled for 20 min at 37 °C with BG-Cy5-CGP **3** (2 μM) and CLIP-Surface 547 **25** (10 μM) (Figure 4A). CLIP-Surface 547 contains the fluorophore DY-547, a good FRET donor for Cy5 (Figure S2, SI). It should be noted that the use of membrane impermeable substrates for the labeling of GABA-Snifit allows us to assemble the sensor exclusively on the cell surface (Figure S3, SI). Perfusion of the cells with buffer containing 1 mM GABA resulted in a decrease in DY-547 fluorescence, an increase in Cy5 fluorescence, and a resulting decrease in the emission ratio ($F_{DY\text{-}547}/F_{Cy5}$) (Figure 4B). Control experiments of cells expressing GABA-Snifit and labeled with BG-Cy5 **6** lacking the $GABA_B$ receptor antagonist did not result in a detectable intensity ratio change upon GABA addition (Figure S4, SI). Furthermore, mock-transfected HEK 293 cells which were incubated with BG-Cy5-CGP **3** (2 μM) and CLIP-Surface 547 **25** (10 μM) did not show any unspecific fluorescent labeling or background fluorescence (Figure S5, SI). In further control experiments GABA-Snifit was perfused with $GABA_B$-unspecific ligands such as glutamate, glycine, aspartate, and others, resulting in no intensity ratio change (Figure S6, SI). This indicates that the observed intensity ratio change of GABA-Snifit labeled with BG-Cy5-CGP **3** is indeed due to a specific replacement of the $GABA_B$ receptor antagonist by GABA and a concomitant switching of GABA-Snifit to an open conformation. The fact that FRET efficiency increases upon sensor opening is noteworthy as previously described Snifits showed a decrease in FRET efficiency upon sensor opening. However, the $GABA_B$ receptor is a heterodimeric transmembrane receptor that is known to form stable dimers of heterodimers.[28] The dimerization was shown to occur at the level of GB1,[34] raising the possibility that the covalently bound antagonist binds to the GB1a of the other heterodimer. Another unique property of GABA-Snifit is that the SNAP-CLIP fusion is separated from the GABA-binding domain by an additional domain, the so-called Sushi domains (Figure 1B), whereas in previously described Snifits SNAP-CLIP was fused directly to the ligand-binding domain. To gain more insights into the sensing mechanism of GABA-Snifit, we compared its FRET efficiency in the open state with those of two other Snifits previously utilized on cell surfaces. These were a Snifit for sulfonamides based on human carbonic anhydrase (HCA-Snifit)[20] and a Snifit for glutamate based on the ionotropic glutamate receptor iGluR5 (Snifit-iGluR5).[21] All three Snifits were expressed in HEK 293 cells and labeled with BG-Cy5 **6** and BC-DY-547 **25**, and the fluorescence emission intensity ratios were measured for all three Snifits under identical instrument settings. Snifits labeled with fluorophores not containing a ligand for the receptor proteins mimic the open state of the sensor. We found that the intensity ratio is similar for all three Snifits (Figure S7, SI). This demonstrates that the dimerization of $GABA_B$ does not influence the FRET efficiency in the open Snifit state. However, the absence of structural information on (dimeric) $GABA_B$ receptor prevents a clarification if sensor closing is due to an inter- or intramolecular interaction. Regardless, our results demonstrate that the GABA-dependent emission ratio change is due to a displacement of the fluorescent antagonist from the GABA binding site.

To determine the concentration range in which GABA-Snifit can be utilized to measure changes in [GABA], we perfused cells expressing GABA-Snifit with different GABA concentrations (Figure 5A) and fitted the corresponding ratio changes to a single-site binding isotherm (eq 4, SI; Figure 5B). These experiments yielded a $K_d^{comp,GABA}$ of 100 ± 10 μM; this constant represents the concentration at which GABA has displaced half of the antagonist from the binding site. It should be noted that the affinity of GABA is lower than its efficacy at $GABA_B$[35] and that in labeled GABA-Snifit GABA competes for binding with tethered $GABA_B$ antagonist. For these reasons, higher GABA concentrations are needed to open the GABA-Snifit than to induce an intracellular calcium response. Different reports indicate that GABA concentrations in brain rise to the

dx.doi.org/10.1021/ja306320s | J. Am. Chem. Soc. 2012, 134, 19026−19034

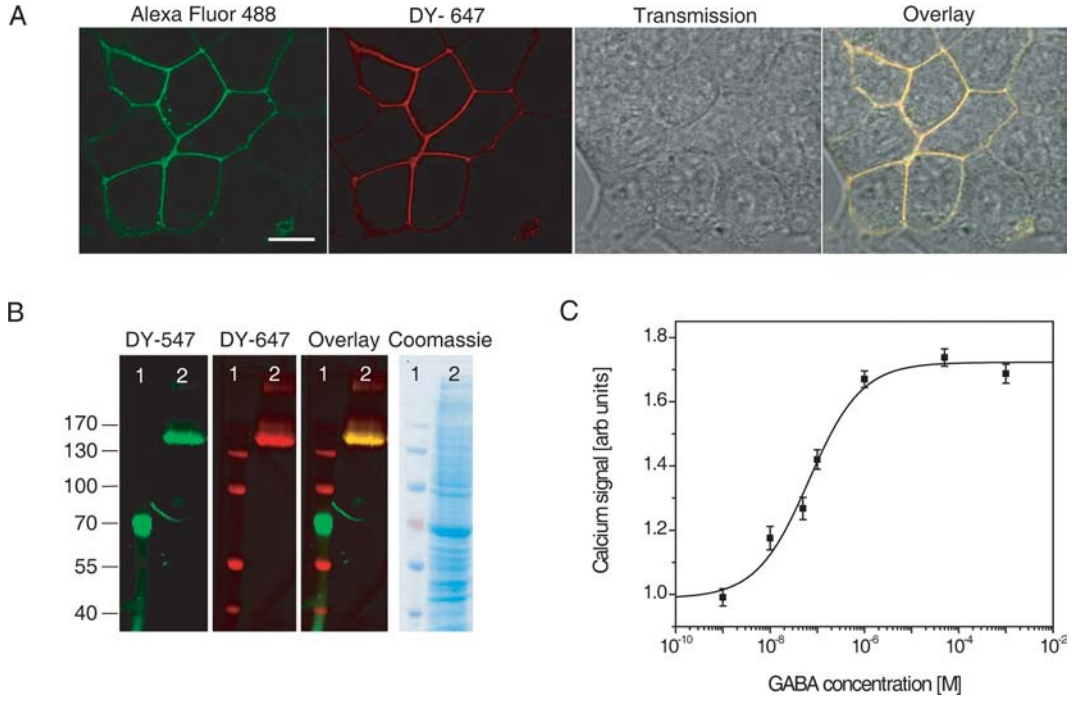

Figure 3. Characterization of GABA-Snifit. (A) Expression of GABA-Snifit on the surface of mammalian cells. SNAP-CLIP-GB1a was labeled on the surface of HEK 293 cells with the dyes Alexa Fluor 488 and DY-647 via their corresponding benzylcytosine (BC)- and benzylguanine (BG)-derivatives. Images were taken using a confocal Zeiss LSM 700 microscope. Scale bar 10 μm. (B) SDS-PAGE and in-gel fluorescence scanning of the labeled sensor protein SNAP-CLIP-GB1a on HEK 293 cell surface and Coomassie staining. Lane 1: MW, lane 2: GABA-Snifit (150 kDa). (C) Calcium dose response generated by increasing concentrations of GABA in HEK 293 cells expressing SNAP-CLIP-GB1a together with GB2 and the chimeric G protein Gqi9. In this experiment GABA-Snifit was not labeled. Data are means ± s.d. of triplicate determinations and representative of three independent experiments.

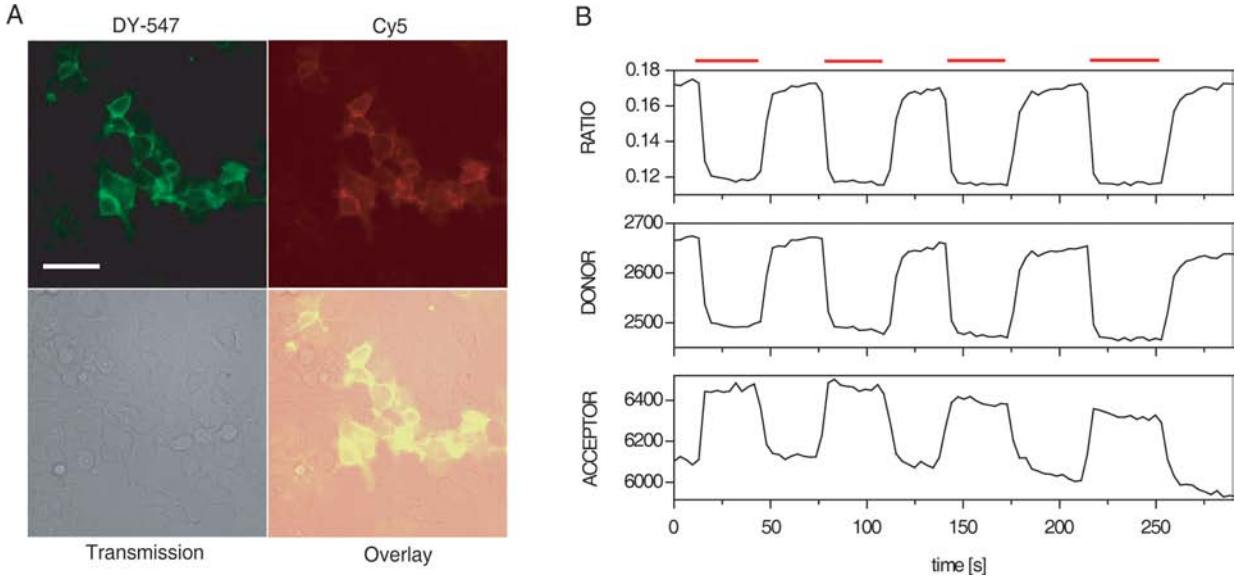

Figure 4. Perfusion experiments for GABA detection on the surface of HEK 293 cells. (A) Donor channel (DY-547), FRET channel (Cy5), and transmission channel of the GABA-Snifit on HEK 293 cells labeled with BC-DY-547 **25** and BG-Cy5-CGP **3**. Scale bar 50 μm. (B) Time course of the intensity ratio of donor emission vs acceptor emission (top), of the donor channel (middle), and the acceptor channel (bottom) upon addition and removal of 1 mM GABA. The red bar indicates the time span of GABA perfusion.

millimolar range and that GABA's half-maximal response (EC_{50}) in brain stem slices of rats is about 20−70 μM.[36] The here measured $K_d^{comp,GABA}$ demonstrates that GABA-Snifit detects GABA in a concentration-dependent manner and that it should be well suited for GABA detection under physiological conditions. By dividing the intensity ratio when no GABA is present and at saturating GABA concentration (eq 2, SI) we obtained a maximum ratio change of $\Delta R_{max} = 1.5 \pm 0.08$ for the DY-547−Cy5 pair. We have observed for other Snifits that the quantum yield (QY: the ratio of photons absorbed to photons emitted through fluorescence) of fluorophores bound to SNAP-tag can slightly decrease in the closed state of the sensor and

dx.doi.org/10.1021/ja306320s | J. Am. Chem. Soc. 2012, 134, 19026−19034

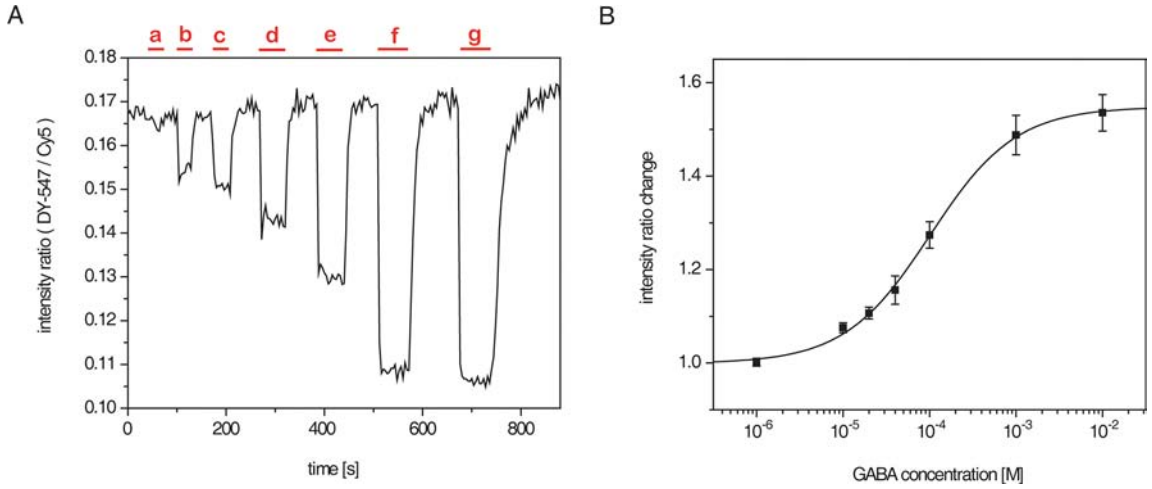

Figure 5. Calibration of GABA-Snifit. (A) Perfusion of GABA-Snifit with increasing GABA concentrations. GABA-Snifit is labeled with BC-DY-547 **25** and BG-Cy5-CGP **3** on the surface of HEK 293 cells and perfused with GABA (a = 1 μM, b = 10 μM, c = 20 μM, d = 40 μM, e = 100 μM, f = 1 mM, g = 10 mM). Shown is the ratio of donor (DY-547) and acceptor (Cy5) emission. (B) GABA titration curve of GABA-Snifit on the surface of HEK 293 cells. Shown is the intensity ratio change $\Delta R = r_{zero}^{DY\text{-}547/Cy5}/r_{GABA}^{DY\text{-}547/Cy5}$ for different GABA concentrations. Data are means ± s.d. of three independent experiments; (n = 15).

that this can contribute to the observed ratio change.[19] To investigate if ΔR_{max} is due to a FRET effect alone or if other factors contribute, we labeled GABA-Snifit with BG-Cy5-CGP **3** but not with CLIP-Surface 547 **25**. We perfused the cells with 1 mM GABA and recorded the emission of Cy5 (Figure S8A,B SI). We observed a decrease in Cy5 fluorescence when the fluorescent antagonist was displaced from the GABA-binding site of GABA-Snifit ($R_{non\text{-}FRET}^{Cy5}$ = 1.07 ± 0.03; eq 3, SI). This environmental effect decreases the total intensity ratio change. To improve the observed ratio change of GABA-Snifit, we labeled the sensor with BG-TMR-CGP **4** as donor fluorophore and CLIP-Surface 647 **24** containing DY-647 as acceptor fluorophore. In this arrangement, a reduced QY of SNAP-bound FRET donor in the closed state should increase the intensity ratio change. As predicted, we found a maximum ratio change of ΔR_{max} = 1.6 ± 0.08 (eq 2, SI) for the TMR/Cy5 pair (Figure S9A, SI and Table 1). This increased maximum ratio change relative to the DY-547/Cy5 pair is due to the environmental effect on the TMR fluorophore ($R_{non\text{-}FRET}^{TMR}$ = 1.08 ± 0.04; eq 3, SI) (Figure S6C,D). Furthermore, control experiments with a derivative of BG-TMR-CGP **4** lacking the $GABA_B$ antagonist (i.e., BG-TMR **7**) did not result in an intensity ratio change upon GABA addition (Figure S10A, SI).

Table 1. Fluorophore Pairs Utilized with GABA-Snifit

SNAP-tag	CLIP-tag	maximum ratio change	environmental effect
BG-Cy5-CGP	BC-DY-547	1.5 ± 0.08	−
BG-Cy5-CGP	BC-Alexa488	1.8 ± 0.06	−
BG-TMR-CGP	BC-DY-647	1.6 ± 0.04	+
BG-TMR-CGP	BC-Alexa488	1.4 ± 0.02	−
BG-Alexa594-CGP	BC-Alexa488	1.3 ± 0.04	−

To further demonstrate the ease with which different FRET pairs can be utilized for GABA-Snifit we labeled it with three additional FRET fluorophore pairs: Alexa Fluor 488/Cy5, Alexa Fluor 488/TMR, and Alexa Fluor 488/Alexa Fluor 594. We found a GABA-dependent intensity ratio change for all fluorophore pairs upon perfusion (Figure S9, SI).

Control experiments for each fluorophore pair confirmed that the observed ratio change is dependent on the presence of covalently attached $GABA_B$ receptor antagonist (Figure S10, SI). The intensity ratio changes for all five different fluorophore pairs tested with GABA-Snifit are summarized in Table 1. The ΔR_{max} varied between 1.3 and 1.8, and the Alexa488/Cy5 pair showed the highest ratio change.

The use of membrane-impermeable dyes results in the exclusive semisynthesis of GABA-Snifit on the cell surface. This prevents interference from sensor protein not fully transported to the cell surface when measuring extracellular GABA concentrations. To visualize the intracellular protein pool of GABA-Snifit we incubated HEK 293 cells expressing GABA-Snifit with a cell-permeable fluorescent SNAP-tag substrate, revealing the presence of a significant intracellular pool of SNAP-CLIP-GB1a (Figure S11, SI). It should be noted that the cell-permeable substrate does not contain the $GABA_B$ antagonist, and thus the intracellular pool of GABA-Snifit does not allow for GABA sensing. In contrast to Snifits, the intra- and extracellular sensor populations of FRET sensors based on autofluorescent proteins can only be discriminated through confocal microscopy, complicating the use of these sensors.

Signal transduction of $GABA_B$ might interfere with the use of GABA-Snifit and/or might result in the internalization of GABA-Snifit. To prevent GPCR signaling after $GABA_B$ receptor activation, we replaced wt-$GABA_B$ with the $GABA_B$ receptor chimera GB1/2[37] (Figure S12A, SI). GB1/2 contains the VFT of GB1a and the 7-TM of GB2. It is able to bind $GABA_B$ receptor ligands but is not able to couple to G proteins. SNAP-CLIP-GB1/2 fusion protein was expressed in HEK 293 cells, and its cell surface expression was confirmed by confocal microscopy (Figure S12B, SI). When SNAP-CLIP-GB1/2 was labeled with BG-Cy5-CGP **3** and CLIP-Surface 547 **25**, we could detect GABA by a decrease in the emission ratio with a ΔR_{max} of 1.4 (Figure S12C, SI). GB2 VFT was reported to increase GB1 VFT affinity for GABA.[38] As this $GABA_B$ domain is missing in the new GABA-Snifit, we observed $K_d^{comp,GABA}$ of 420 ± 50 μM upon perfusion with different [GABA] (Figure

dx.doi.org/10.1021/ja306320s | J. Am. Chem. Soc. 2012, 134, 19026−19034

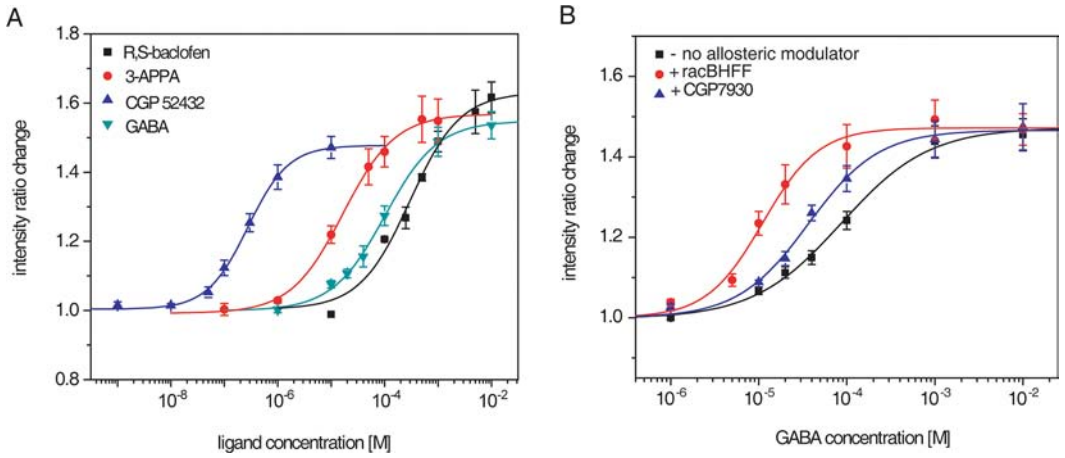

Figure 6. Titration curves of SNAP-CLIP-GB1a on the surface of HEK 293 cells with different $GABA_B$ receptor ligands. GABA-Snifit is labeled with BC-DY-547 **25** and BG-Cy5-CGP **3** on the surface of HEK 293 cells and perfused with increasing concentrations of ligands. (A) Intensity ratio change $\Delta R = r_{zero}^{DY\text{-}547/Cy5}/r_{ligand}^{DY\text{-}547/Cy5}$ for different concentrations of the agonists *R,S*-baclofen (black squares), GABA (cyan triangles), 3-APPA (red circles), and for the antagonist CGP 52432 (blue triangles). (B) Intensity ratio change $\Delta R = r_{zero}^{DY\text{-}547/Cy5}/r_{GABA}^{DY\text{-}547/Cy5}$ for different GABA concentrations in the absence of PAMs (black squares) and the presence of the PAMs CGP 7930 (blue triangles) or rac-BHFF (red circles). Data are means ± s.d. of three independent experiments ($n \geq 18$).

S12D SI) compared to the previously described $K_d^{comp,GABA}$ of 100 ± 10 μM.

Functional tests with SNAP-CLIP-GB1/2 and the chimeric G protein Gqi9 showed no increase in cytosolic calcium concentrations upon addition of GABA (Figure S12E, SI). This demonstrates that SNAP-CLIP-GB1/2 is suitable as GABA Snifit. It senses GABA on the cell surface in a higher concentration range and is nonfunctional with respect to G protein coupling. GABA-Snifit based on GB1/2 is therefore suitable for sensor applications where cell signaling has to be avoided.

The release of GABA from neurons takes place over a period of ~200 ms,[39] and the temporal resolution of any GABA sensor ideally should be in a similar range. Our previous experiments with other Snifits[19−21] suggest that the kinetics of the opening and closing of GABA-Snifit should be determined by the dissociation rate constant (k_{off}) of the tethered fluorescent antagonist and GABA, respectively. A k_{off} of 5.8 s^{-1} has been reported for the dissociation of GABA from $GABA_B$.[40] We attempted to determine the rate of sensor opening and closing through GABA perfusion experiments. The measured opening rate of the sensor ($k_{opening}$ = 0.68 ± 0.17 s^{-1}; obtained by fitting the change in emission ratio to a single exponential function; SI, eq 5 and Figure S13A) was similar to the speed with which the bath solution inside the perfusion chamber could be exchanged ($k_{perfusion}$ = 0.77 ± 0.04 s^{-1}; Figure S14, SI). As observed for sensor opening, the measured rate for sensor closing upon GABA removal was at least partially determined by the rate of GABA removal from the perfusion chamber ($k_{closing}$ = 0.35 ± 0.14 s^{-1}; obtained by fitting the change in emission ratio to a single exponential function; SI eq 6 and Figure S13B). In conclusion, the temporal resolution of GABA-Snifit is in the range of seconds, but more sophisticated experiments are needed to determine if GABA concentration changes in the range of milliseconds can be measured.

Characterization of $GABA_B$ Receptor Agonists, Antagonists, and Allosteric Modulators through GABA-Snifit. The pharmacological manipulation of $GABA_B$ receptors is of interest for the treatment of a wide variety of neurological diseases and psychiatric disorders.[41] The only synthetic ligand currently in clinical use is the agonist Baclofen (4-amino-3-(4-chlorophenyl)butanoic acid - Lioresal). GABA-Snifit could be employed in drug research for the characterization of the affinity of synthetic $GABA_B$ receptor agonists and antagonists as the binding of such ligands to the orthosteric site of $GABA_B$ receptor should switch GABA-Snifit to its open conformation. We characterized the interaction of GABA-Snifit with the known agonists *R,S*-baclofen[42] and 3-APPA (3-aminopropyl-phosphinic acid)[43] as well as the antagonist CGP 52432 ([3-[[(3,4-dichlorophenyl)methyl]amino]propyl](diethoxy-methyl)phosphinic acid).[44] All three ligands were able to open the sensor (Figure S15, SI), and by titrating the sensor with different ligand concentrations and fitting the data to a single-site binding isotherm (SI eq 4) we obtained $K_d^{comp,baclofen}$ = 300 ± 60 μM, $K_d^{comp,APPA}$ = 20 ± 1.7 μM, and $K_d^{comp,CGP52432}$ = 280 ± 20 nM (Figure 6A). $K_d^{comp,ligand}$ reflects the affinity of each ligand for the $GABA_B$ receptor. The K_d^{comp} values of *R,S*-baclofen and 3-APPA are in agreement with the reported 15-fold difference between their $GABA_B$ receptor affinities (35 nM for *R,S*-baclofen and 2.4 nM for 3-APPA; inhibition of binding of [^{3}H]-baclofen to cat cerebellum).[45] In contrast, according to our K_d^{comp} values, the $GABA_B$ affinity of the antagonist CGP 52432 is 70-fold higher than that of 3-APPA, whereas its reported affinity on brain membranes is 11 times lower (55 nM for CGP 52432 and 5 nM for 3-APPA; inhibition of binding of [^{3}H]-APPA to rat cerebral cortex membranes).[29] We speculate that this discrepancy is due to the different assay systems employed: GABA-Snifit measures the affinity of a ligand for the heterologously expressed $GABA_B$ receptor consisting of GB1a and GB2 in HEK 293 cells, whereas in previous reports the affinity of a ligand for the ensemble of $GABA_B$ receptors was measured in preparations of brain membranes. It was shown for 3-APPA that agonist affinities to native $GABA_B$ receptors differ from those measured for recombinant $GABA_B$.[46] Furthermore $GABA_B$ receptor isoforms may be pharmacologically heterogenic in vivo, and some show insensitivity toward CGP 52432.[47] Thus, GABA-Snifit can be utilized in drug discovery to characterize the specific binding affinity of $GABA_B$ agonists or antagonists, but the measured affinity does not necessarily reflect the affinities of such ligands in vivo.

dx.doi.org/10.1021/ja306320s | J. Am. Chem. Soc. 2012, 134, 19026−19034

Allosteric modulators of $GABA_B$ receptors bind to $GABA_B$ outside its orthosteric site, thereby altering the binding affinity and biological activity of agonists or antagonists.[48] To test if GABA-Snifit can sense the activity of allosteric modulators of the $GABA_B$ receptor we used the positive allosteric modulators (PAMs) CGP 7930 (2,6-di-*tert*-butyl-4-(3-hydroxy-2,2-dimethyl-propyl)-phenol)[49] and rac-BHFF ((*R*,*S*)-5,7-di-*tert*-butyl-3-hydroxy-3-trifluoromethyl-3*H*-benzofuran-2-one).[50] CGP 7930 and rac-BHFF are known to increase the affinity of $GABA_B$ receptor agonists but not antagonists, presumably by binding to the heptahelical domain of GB2.[51] The addition of CGP 7930 (30 μM) or rac-BHFF (10 μM) in GABA titration experiments of GABA-Snifit reduced $K_d^{comp,GABA}$ from 90 μM ± 10 μM to 30 μM ± 3 μM with CGP 7930 and to 10 μM ± 1 μM with rac-BHFF (Figure 6B). The observed 3-fold increase in agonist affinity is in agreement with previously published data on the CGP 7930-dependence of [^{3}H]3-APPA binding to $GABA_B$ receptors in rat cortical membranes.[49] For rac-BHFF a nonselective GABA-binding assay is reported where rac-BHFF enhanced [^{3}H]-GABA binding in rat cerebral cortex by 2-fold.[50] However, rac-BHFF is 20-fold more potent than CGP 7930 in increasing GABA efficacy at $GABA_B$ receptors.[48] Our data confirm that rac-BHFF is a more potent PAM than CGP 7930. In conclusion, GABA-Snifit is capable of sensing the activity of positive allosteric modulators of $GABA_B$, broadening its use for applications in drug discovery. These results also demonstrate that the interaction of ligands other than GABA with GABA-Snifit can interfere with GABA sensing.

DISCUSSION

GABA-Snifit is the first fluorescent ratiometric sensor for measuring GABA concentrations on the surface of live cells. GABA-Snifit senses GABA in a physiologically relevant concentration range from low μM to mM with high spatiotemporal resolution. Considering (i) the ubiquitous role of GABA in neurobiology, embryonic development and adult neurogenesis, and (ii) the absence of other suitable sensors for measuring GABA concentrations with appropriate spatiotemporal resolution, GABA-Snifit should become a valuable research tool in biology. An important feature of GABA-Snifit is its modular design which facilitates an adaption of the sensor toward a particular application. For example, by exchanging its underlying fluorophores different FRET pairs can be readily generated. This flexibility is important when GABA-Snifit will be used simultaneously with other, less flexible fluorescent sensors in multiplexing experiments. Furthermore, previous studies on the structure–activity relationship (SAR) of $GABA_B$ antagonist CGP 51783 suggest how to modify the tethered ligand to either improve or decrease its affinity.[32] Changing the affinity of the tethered ligand of GABA-Snifit would shift the concentration range at which the sensor could be used.

Another application of GABA-Snifit is to sense the affinity of synthetic ligands of $GABA_B$. Such ligands can be agonists, antagonists, or allosteric modulators, all of which are of importance in drug research.

GABA-Snifit might also be used for studying the function of $GABA_B$. The tethering of an antagonist to GABA-Snifit locks the receptor in an inactive conformation until GABA concentrations rise to μmolar levels. As the activation of GABA-Snifit by GABA or other agonists results in an emission ratio change, a simultaneous visualization of receptor activation and internal signaling events for which appropriate fluorescent sensors are available should be possible. Furthermore, locking $GABA_B$ in a defined conformation through a tethered ligand might facilitate structural studies. A synthetic agonist covalently tethered to $\beta(2)$ adrenergic receptor was shown to stabilize the receptor in an active conformation and facilitate its crystallization.[52]

Another important aspect of this work is the demonstration that GPCRs can act as binding proteins to generate fluorescent ratiometric sensors for applications on cell surfaces on the basis of the Snifit concept. Hundreds of different GPCRs have been identified, and their ligands include neurotransmitters, hormones, odorants, and pheromones. GABA-Snifit might therefore be the first example of a family of GPCR-based Snifits for biologically important analytes. It has been shown for more than 20 GPCRs that they can be functionally expressed as N-terminal SNAP-tag fusion proteins,[53−55] and synthetic ligands for numerous GPCRs have been described that could serve as starting points for the design of tethered fluorescent ligands.[56,57]

CONCLUSION

We have introduced the first fluorescent sensor for the important neurotransmitter GABA based on the $GABA_B$ receptor. The sensor should become a powerful tool for studying the role of GABA in biology and for quantifying the relative binding affinities of $GABA_B$ receptor agonists, antagonists and the effect of allosteric modulators. Furthermore, GABA-Snifit should serve as blueprint for the generation of other GPCR-based fluorescent sensors for biologically relevant extracellular metabolites.

METHODS

Synthesis. The detailed synthetic procedures and compound characterizations are described in the SI.

Cell Culture and Transfection. HEK 293 cells were grown on polyornithine-coated glass coverslips (Ø 15 mm) in DMEM Glutamax medium (Lonza) supplemented with 10% fetal bovine serum (Lonza). Transient transfection was performed using Lipofectamine 2000 (Invitrogen) and a total of 0.75 μg DNA (SNAP-CLIP-GB1a/GB2 = 1:1) and a DNA/lipofectamine ratio of 0.4.

SNAP- and CLIP-Tag Labeling on the Surface of Live Mammalian Cells. At 24–48 h after transfection HEK 293 cells were labeled by incubation with a solution of 2 μM of the fluorescent O^6-benzylguanine (BG) and 10 μM of the fluorescent O^2-benzylcytosine (BC) derivatives in Hank's buffered salt solution (HBSS; Lonza) complemented with 10 mg/mL BSA (Sigma-Aldrich) for 20 min at 37 °C followed by four washing steps with HBSS.

Confocal Microscopy. Twenty-four hours after transfection HEK 293 cells were labeled with BC-Alexa Fluor 488 **23** and SNAP-Surface 647 (New England Biolabs) and imaged using a Zeiss LSM 700 confocal microscope equipped with a 40 × plan Apochromat 1.3 numerical aperture (NA) oil immersion objective lens. The imaging was performed using a 488 nm laser line for excitation of Alexa Fluor 488 and a 639 nm laser line for excitation of DY-647. Fluorescence was collected at 510–560 nm and at 650–700 nm for BC-Alexa Fluor 488 and DY-647, respectively. The settings for scanning were: × 2 zoom, image format 1024 × 1024 pixels, pinhole 1 Airy unit (AU), average 16 frames.

Wide-Field Microscopy and Live Cell FRET Imaging. Perfusion experiments were performed by transferring the glass coverslips with the labeled HEK 293 cells to a Warner imaging chamber (RC-20) and perfusing it with HBSS or HBSS containing different $GABA_B$ receptor ligands (GABA (Sigma-Aldrich); *R*,*S*-Baclofen, 3-APPA, CGP 52432 and CGP 7930 (Abcam)) gravity-fed at a flow rate of 0.5 mL/min. Imaging of sensors time-course experiments was performed using a Leica LAS AF 7000 wide-field microscope equipped with a 40 × plan Apochromat 1.25 NA oil immersion objective lens and a xenon arc

lamp. For recording each frame the donor and the FRET channel were measured consecutively with an interval between 10 and 0.7 s, depending on the experiment. The image size was 293 μm × 293 μm if not stated otherwise. The following filter sets were used for the FRET ratio imaging: for DY-547/Cy5, excitation at 530 nm (bandwidth 35 nm), emission at 580 nm (bandwidth 40 nm) (DY-547) and at 700 nm (bandwidth 72 nm) (Cy5); for Alexa Fluor 488/Cy5, excitation at 470 nm (bandwidth 40 nm), emission at 580 nm (bandwidth 40 nm) (Alexa Fluor 488) and at 700 nm (bandwidth 72 nm) (Cy5); for Alexa Fluor 488/TMR, excitation at 470 nm (bandwidth 40 nm), emission at 520 nm (bandwidth 40 nm) (Alexa Fluor 488) and at 605 nm (bandwidth 70 nm) (TMR); for Alexa Fluor 488/Alexa Fluor 594, excitation at 470 nm (bandwidth 40 nm), emission at 520 nm (bandwidth 40 nm) (Alexa Fluor 488) and at 632 nm (bandwidth 60 nm) (Alexa Fluor 594).

SDS-PAGE Analysis. After 72 h of transient protein expression transfected HEK 293 cells were labeled with 2 μM SNAP-Surface 647 and 10 μM CLIP-Surface 547 (New England Biolabs) for 20 min at 37 °C. The labeled cells were lysed by rocking them for 45 min at 4 °C with RIPA buffer (50 mM TrisHCl, pH 7.4, 150 mM NaCl, 1% Igepal CA-630, 0.5% sodium deoxycholate, 0.1% SDS, protease inhibitor cocktail tablets (Roche) in presence of 100 μM SNAP-Cell Block and CLIP-Cell Block (New England Biolabs). The supernatant was cleared by spinning the cells at 10000 rpm at 4 °C for 30 min, incubated for 1 h at RT with SDS loading buffer and analyzed on a 7.5% SDS-polyacrylamide gel by electrophoresis (SDS-PAGE) and in-gel fluorescence scanning.

Intracellular Calcium Measurements. HEK 293 cells were reversely transfected with plasmids encoding SNAP-CLIP-GB1a together with GB2 and a chimeric protein Gqi9 using Lipofectamine 2000 (Invitrogen) seeding them in 96-well clear-bottom black-well plates (Corning) pretreated with poly ornithin (Sigma-Aldrich) at 100,000 cells/well. Forty-eight hours after transfection intracellular calcium measurements were performed as previously described[28] after addition of various GABA concentrations.

■ ASSOCIATED CONTENT

Ⓢ Supporting Information

Synthetic procedures, protein sequences, additional methods, and additional figures for the characterization of GABA-Snifit on the cell surface. This material is available free of charge via the Internet at http://pubs.acs.org.

■ AUTHOR INFORMATION

Corresponding Author

kai.johnsson@epfl.ch

Present Addresses

[†]Plateforme ARPEGE, Institut de Génomique Fonctionnelle, IGF NORD, Bureau 225, 141, rue de la Cardonille, 34094 Montpellier, France.

[‡]Laboratory of Chemical Biology and Molecular Imaging, University of Tokyo, 7-3-1 Hongo, Bunkyo-ku, Tokyo 113-0033, Japan.

Notes

The authors declare no competing financial interest.

■ ACKNOWLEDGMENTS

This work was supported by the Swiss National Science Foundation, the European Research Training Network ENEFP (A.M.), and a JSPS Research Fellowship for Research Abroad (K.U.). We thank Dr. W. Froestl, Dr. G. Lukinavicius, Dr. M. Brun, and R. Griss for valuable discussions, Dr. J. P. Pin for the $GABA_B$ receptor and the Gqi9 plasmids, Dr. C. Trefzer for technical assistance, and N. Tappin for corrections of the manuscript.

■ REFERENCES

(1) Roberts, E. *GABA and Benzodiazepine Receptors*; CRC Press: Boca Raton, FL, 1988.

(2) Paredes, R. G.; Agmo, A. *Neurosci. Biobehav. Rev.* **1992**, *16*, 145−170.

(3) Owens, D. F.; Kriegstein, A. R. *Nat. Rev. Neurosci.* **2002**, *3*, 715−727.

(4) Erdo, S. L.; Wolff, J. R. *J. Neurochem.* **1990**, *54*, 363−372.

(5) Rothman, D. L.; Petroff, O. A. C.; Behar, K. L.; Mattson, R. H. *Proc. Natl. Acad. Sci. U.S.A.* **1993**, *90*, 5662−5666.

(6) Yoon, J. H.; Maddock, R. J.; Rokem, A.; Silver, M. A.; Minzenberg, M. J.; Ragland, J. D.; Carter, C. S. *J. Neurosci.* **2010**, *30*, 3777−3781.

(7) Kehr, J. *J. Chromatogr., B.* **1998**, *708*, 49−54.

(8) Buck, K.; Voehringer, P.; Ferger, B. *J. Neurosci. Methods* **2009**, *182*, 78−84.

(9) Niwa, O.; Kurita, R.; Horiuchi, T.; Torimitsu, K. *Anal. Chem.* **1998**, *70*, 89−93.

(10) Wang, T. T.; Muthuswamy, J. *Anal. Chem.* **2008**, *80*, 8576−8582.

(11) Frommer, W. B.; Davidson, M. W.; Campbell, R. E. *Chem. Soc. Rev.* **2009**, *38*, 2833−2841.

(12) Okumoto, S.; Looger, L. L.; Micheva, K. D.; Reimer, R. J.; Smith, S. J.; Frommer, W. B. *Proc. Natl. Acad. Sci. U.S.A.* **2005**, *102*, 8740−8745.

(13) Fehr, M.; Okumoto, S.; Deuschle, K.; Lager, I.; Looger, L. L.; Persson, J.; Kozhukh, L.; Lalonde, S.; Frommer, W. B. *Biochem. Soc. Trans.* **2005**, *33*, 287−290.

(14) Honda, A.; Adams, S. R.; Sawyer, C. L.; Lev-Ram, V.; Tsien, R. Y.; Dostmann, W. R. G. *Proc. Natl. Acad. Sci. U.S.A.* **2001**, *98*, 2437−2442.

(15) Nagai, Y.; Miyazaki, M.; Aoki, R.; Zama, T.; Inouye, S.; Hirose, K.; Iino, M.; Hagiwara, M. *Nat. Biotechnol.* **2000**, *18*, 313−316.

(16) Romoser, V. A.; Hinkle, P. M.; Persechini, A. *J. Biol. Chem.* **1997**, *272*, 13270−13274.

(17) Cicchetti, G.; Biernacki, M.; Farquharson, J.; Allen, P. G. *Biochemistry* **2004**, *43*, 1939−1949.

(18) Bogner, M.; Ludewig, U. *J. Fluoresc.* **2007**, *17*, 350−360.

(19) Brun, M. A.; Tan, K. T.; Nakata, E.; Hinner, M. J.; Johnsson, K. *J. Am. Chem. Soc.* **2009**, *131*, 5873−5884.

(20) Brun, M. A.; Griss, R.; Reymond, L.; Tan, K. T.; Piguet, J.; Peters, R. J.; Vogel, H.; Johnsson, K. *J. Am. Chem. Soc.* **2011**, 16235−16242.

(21) Brun, M. A.; Tan, K. T.; Griss, R.; Kielkowska, A.; Reymond, L.; Johnsson, K. *J. Am. Chem. Soc.* **2012**, *134*, 7676−7678.

(22) Keppler, A.; Gendreizig, S.; Gronemeyer, T.; Pick, H.; Vogel, H.; Johnsson, K. *Nat. Biotechnol.* **2003**, *21*, 86−89.

(23) Gautier, A.; Juillerat, A.; Heinis, C.; Correa, I. R.; Kindermann, M.; Beaufils, F.; Johnsson, K. *Chem. Biol.* **2008**, *15*, 128−136.

(24) Blein, S.; Ginham, R.; Uhrin, D.; Smith, B. O.; Soares, D. C.; Veltel, S.; McIlhinney, R. A.; White, J. H.; Barlow, P. N. *J. Biol. Chem.* **2004**, *279*, 48292−48306.

(25) Biermann, B.; Ivankova-Susankova, K.; Bradaia, A.; Aziz, S. A.; Besseyrias, V.; Kapfhammer, J. P.; Missler, M.; Gassmann, M.; Bettler, B. *J. Neurosci.* **2010**, *30*, 1385−1394.

(26) Jones, K. A.; Borowsky, B.; Tamm, J. A.; Craig, D. A.; Durkin, M. M.; Dai, M.; Yao, W. J.; Johnson, M.; Gunwaldsen, C.; Huang, L. Y.; Tang, C.; Shen, Q.; Salon, J. A.; Morse, K.; Laz, T.; Smith, K. E.; Nagarathnam, D.; Noble, S. A.; Branchek, T. A.; Gerald, C. *Nature* **1998**, *396*, 674−679.

(27) Duthey, B.; Caudron, S.; Perroy, J.; Bettler, B.; Fagni, L.; Pin, J. P.; Prezeau, L. *J. Biol. Chem.* **2002**, *277*, 3236−3241.

(28) Maurel, D.; Comps-Agrar, L.; Brock, C.; Rives, M. L.; Bourrier, E.; Ayoub, M. A.; Bazin, H.; Tinel, N.; Durroux, T.; Prezeau, L.; Trinquet, E.; Pin, J. P. *Nat. Methods* **2008**, *5*, 561−567.

(29) Froestl, W. *Adv. Pharmacol.* **2010**, *58*, 19−62.

(30) Kaupmann, K.; Huggel, K.; Heid, J.; Flor, P. J.; Bischoff, S.; Mickel, S. J.; McMaster, G.; Angst, C.; Bittiger, H.; Froestl, W.; Bettler, B. *Nature* **1997**, *386*, 239−246.

(31) Froestl, W.; Bettler, B.; Bittiger, H.; Heid, J.; Kaupmann, K.; Mickel, S. J.; Strub, D. *Neuropharmacology* **1999**, *38*, 1641−1646.
(32) Froestl, W.; Mickel, S. J.; von Sprecher, G.; Bittiger, H.; Olpe, H.-R. *Pharmacol. Commun.* **1992**, *2*, 52−56.
(33) Franek, M.; Pagano, A.; Kaupmann, K.; Bettler, B.; Pin, J. P.; Blahos, J. *Neuropharmacology* **1999**, *38*, 1657−1666.
(34) Comps-Agrar, L.; Kniazeff, J.; Norskov-Lauritsen, L.; Maurel, D.; Gassmann, M.; Gregor, N.; Prezeau, L.; Bettler, B.; Durroux, T.; Trinquet, E.; Pin, J. P. *EMBO J.* **2011**, *30*, 2336−2349.
(35) Kniazeff, J.; Galvez, T.; Labesse, G.; Pin, J. P. *J. Neurosci.* **2002**, *22*, 7352−7361.
(36) Grabauskas, G. *Neurosci. Lett.* **2005**, *373*, 10−15.
(37) Galvez, T.; Duthey, B.; Kniazeff, J.; Blahos, J.; Rovelli, G.; Bettler, B.; Prezeau, L.; Pin, J. P. *EMBO J.* **2001**, *20*, 2152−2159.
(38) Liu, J. F.; Maurel, D.; Etzol, S.; Brabet, I.; Ansanay, H.; Pin, J. P.; Rondard, P. *J. Biol. Chem.* **2004**, *279*, 15824−15830.
(39) Connors, B. W.; Malenka, R. C.; Silva, L. R. *J. Physiol.* **1988**, *406*, 443−468.
(40) Chu, D. C.; Albin, R. L.; Young, A. B.; Penney, J. B. *Neuroscience* **1990**, *34*, 341−357.
(41) Marshall, F. H. *J. Mol. Neurosci.* **2005**, *26*, 169−176.
(42) Hill, D. R.; Bowery, N. G. *Nature* **1981**, *290*, 149−152.
(43) Ong, J.; Harrison, N. L.; Hall, R. G.; Barker, J. L.; Johnston, G. A. R.; Kerr, D. I. B. *Brain Res.* **1990**, *526*, 138−142.
(44) Lanza, M.; Fassio, A.; Gemignani, A.; Bonanno, G.; Raiteri, M. *Eur. J. Pharmacol.* **1993**, *237*, 191−195.
(45) Froestl, W.; Mickel, S. J.; Hall, R. G.; von Sprecher, G.; Strub, D.; Baumann, P. A.; Brugger, F.; Gentsch, C.; Jaekel, J.; Olpe, H. R.; et al. *J. Med. Chem.* **1995**, *38*, 3297−3312.
(46) Hirst, W. D.; Babbs, A. J.; Green, A.; Minton, J. A.; Shaw, T. E.; Wise, A.; Rice, S. Q.; Pangalos, M. N.; Price, G. W. *Biochem. Pharmacol.* **2003**, *65*, 1103−1113.
(47) Bonanno, G.; Fassio, A.; Schmid, G.; Severi, P.; Sala, R.; Raiteri, M. *Br. J. Pharmacol.* **1997**, *120*, 60−64.
(48) Urwyler, S. *Pharmacol. Rev.* **2011**, *63*, 59−126.
(49) Urwyler, S.; Mosbacher, J.; Lingenhoehl, K.; Heid, J.; Hofstetter, K.; Froestl, W.; Bettler, B.; Kaupmann, K. *Mol. Pharmacol.* **2001**, *60*, 963−971.
(50) Malherbe, P.; Masciadri, R.; Norcross, R. D.; Knoflach, F.; Kratzeisen, C.; Zenner, M. T.; Kolb, Y.; Marcuz, A.; Huwyler, J.; Nakagawa, T.; Porter, R. H.; Thomas, A. W.; Wettstein, J. G.; Sleight, A. J.; Spooren, W.; Prinssen, E. P. *Br. J. Pharmacol.* **2008**, *154*, 797−811.
(51) Binet, V.; Brajon, C.; Le Corre, L.; Acher, F.; Pin, J. P.; Prezeau, L. *J. Biol. Chem.* **2004**, *279*, 29085−29091.
(52) Rosenbaum, D. M.; Zhang, C.; Lyons, J. A.; Holl, R.; Aragao, D.; Arlow, D. H.; Rasmussen, S. G.; Choi, H. J.; Devree, B. T.; Sunahara, R. K.; Chae, P. S.; Gellman, S. H.; Dror, R. O.; Shaw, D. E.; Weis, W. I.; Caffrey, M.; Gmeiner, P.; Kobilka, B. K. *Nature* **2011**, *469*, 236−240.
(53) Zwier, J. M.; Roux, T.; Cottet, M.; Durroux, T.; Douzon, S.; Bdioui, S.; Gregor, N.; Bourrier, E.; Oueslati, N.; Nicolas, L.; Tinel, N.; Boisseau, C.; Yverneau, P.; Charrier-Savournin, F.; Fink, M.; Trinquet, E. *J. Biomol. Screen.* **2010**, *15*, 1248−1259.
(54) Delille, H. K.; Becker, J. M.; Burkhardt, S.; Bleher, B.; Terstappen, G. C.; Schmidt, M.; Meyer, A. H.; Unger, L.; Marek, G. J.; Mezler, M. *Neuropharmacology* **2012**, *62*, 2184−2191.
(55) Leyris, J. P.; Roux, T.; Trinquet, E.; Verdie, P.; Fehrentz, J. A.; Oueslati, N.; Douzon, S.; Bourrier, E.; Lamarque, L.; Gagne, D.; Galleyrand, J. C.; M'Kadmi, C.; Martinez, J.; Mary, S.; Baneres, J. L.; Marie, J. *Anal. Biochem.* **2011**, *408*, 253−262.
(56) Middleton, R. J.; Kellam, B. *Curr. Opin. Chem. Biol.* **2005**, *9*, 517−525.
(57) Kuder, K.; Kiec-Kononowicz, K. *Curr. Med. Chem.* **2008**, *15*, 2132−2143.